

Adaptive Canceller Limitations Due to Frequency Mismatch Errors

KARL GERLACH

*Radars Techniques Branch
Radars Division*

January 2, 1986



NAVAL RESEARCH LABORATORY
Washington, D.C.

SECURITY CLASSIFICATION OF THIS PAGE

REPORT DOCUMENTATION PAGE				
1a. REPORT SECURITY CLASSIFICATION UNCLASSIFIED		1b. RESTRICTIVE MARKINGS		
2a. SECURITY CLASSIFICATION AUTHORITY		3. DISTRIBUTION / AVAILABILITY OF REPORT Approved for public release; distribution is unlimited.		
2b. DECLASSIFICATION / DOWNGRADING SCHEDULE				
4. PERFORMING ORGANIZATION REPORT NUMBER(S) NRL Report 8949		5. MONITORING ORGANIZATION REPORT NUMBER(S)		
6a. NAME OF PERFORMING ORGANIZATION Naval Research Laboratory	6b. OFFICE SYMBOL (If applicable)	7a. NAME OF MONITORING ORGANIZATION Naval Electronic Systems Command		
6c. ADDRESS (City, State, and ZIP Code) Washington, DC 20375-5000		7b. ADDRESS (City, State, and ZIP Code) Washington, DC 20360		
8a. NAME OF FUNDING / SPONSORING ORGANIZATION Naval Electronic Systems Command	8b. OFFICE SYMBOL (If applicable)	9. PROCUREMENT INSTRUMENT IDENTIFICATION NUMBER		
8c. ADDRESS (City, State, and ZIP Code) Washington, DC 20360		10. SOURCE OF FUNDING NUMBERS		
		PROGRAM ELEMENT NO. G2712N	PROJECT NO.	TASK NO. XF12-141-100
				WORK UNIT ACCESSION NO. DN380-101
11. TITLE (Include Security Classification) Adaptive Cancellor Limitations Due to Frequency Mismatch Errors				
12. PERSONAL AUTHOR(S) Gerlach, Karl R.				
13a. TYPE OF REPORT Interim	13b. TIME COVERED FROM _____ TO _____	14. DATE OF REPORT (Year, Month, Day) 1986 January 2	15. PAGE COUNT 33	
16. SUPPLEMENTARY NOTATION				
17. COSATI CODES			18. SUBJECT TERMS (Continue on reverse if necessary and identify by block number)	
FIELD	GROUP	SUB-GROUP	Adaptive filter	
			Radar	
			Adaptive cancellation	
19. ABSTRACT (Continue on reverse if necessary and identify by block number)				
<p>The effects of frequency mismatch errors on adaptive cancellers are investigated. Frequency mismatch errors occur because of errors in the synthesis process of the bandpass filters designed to be identical which are in each input channel. These frequency mismatches among the channels result in cancellation degradation. Tapped delay line transversal filters can be used to compensate for these frequency mismatches and thus improve cancellation performance. A pole/zero error model of the filters is developed whereby closed form solutions of the maximum achievable cancellation are obtained. This cancellation is a function of the order of the ideally matched frequency filters, the number of time delay taps in the compensating transversal filter, the bandwidth-tapped time delay product, and the constraints on these parameters. A design procedure is outlined for "optimizing" the canceller with respect to these parameters and their constraints. Specifically, results are presented for when the input filters are the Butterworth type. It is shown that an arbitrarily low output noise residue cannot be achieved by arbitrarily increasing the number of time delay taps.</p>				
20. DISTRIBUTION / AVAILABILITY OF ABSTRACT <input checked="" type="checkbox"/> UNCLASSIFIED/UNLIMITED <input type="checkbox"/> SAME AS RPT. <input type="checkbox"/> DTIC USERS		21. ABSTRACT SECURITY CLASSIFICATION UNCLASSIFIED		
22a. NAME OF RESPONSIBLE INDIVIDUAL Karl R. Gerlach		22b. TELEPHONE (Include Area Code) (202) 767-4873	22c. OFFICE SYMBOL 5320	

CONTENTS

I. INTRODUCTION	1
II. POLE/ZERO ERROR MODEL	2
III. RESIDUE DERIVATION	5
IV. A SPECIAL CASE: THE BUTTERWORTH FILTER	9
V. RESULTS	11
VI. SUMMARY AND CONCLUSIONS	20
VII. REFERENCES	21
APPENDIX A – Derivation of Equations (3.30) to (3.34)	22
APPENDIX B – Evaluation of Integrals	25

ADAPTIVE CANCELLER LIMITATIONS DUE TO FREQUENCY MISMATCH ERRORS

I. INTRODUCTION

An adaptive canceller combines auxiliary channels of data with a main channel of data in such a way so as to minimize the main channel output noise power residue. Hence, this is an effective way of eliminating unwanted data (or noise) from a main channel (the information channel) by inputting correlated data from auxiliary channels. Mismatch errors of any kind between channels of an adaptive canceller can cause a reduction in the achievable cancellation ratio. These mismatch errors can include small time delay differences, in-phase (I) and quadrature-phase (Q) imbalances, strobing errors, and frequency mismatch errors among the various channels. For a radar or communications digital canceller, many of these errors occur due to the radio frequency (RF)-to-intermediate frequency (IF)-to-baseband-to-sample and hold (S+H)-to-analog-to-digital (A/D) chain which is present in each channel. If any link of this chain is not identical among the channels, there are mismatch errors which cause the canceller performance to degrade.

In this report, we concern ourselves with just frequency mismatch errors. Other research in this area can be found in Ref. 1. To compensate for frequency mismatch errors, often adaptive digital transversal filters are inserted into the auxiliary channels. Figure 1.1 illustrates a two channel compensated adaptive canceller. Here, we have two signals $y_M(t)$ and $y_A(t)$ inputted into the main and auxiliary channels, respectively. These signals will normally pass through bandpass filters in each channel. The bandwidth of these filters is set equal to the bandwidth of the desired signal. Let the frequency transfer functions (FTF) of the main and auxiliary channels be $H_M(j\omega)$ and $H_A(j\omega)$, respectively. Normally, both of these FTFs are designed to be equal to some desired FTF: $H(j\omega)$. However, because of inaccuracies in the filter synthesis process, $H_M(j\omega)$ and $H_A(j\omega)$ may not be equal.

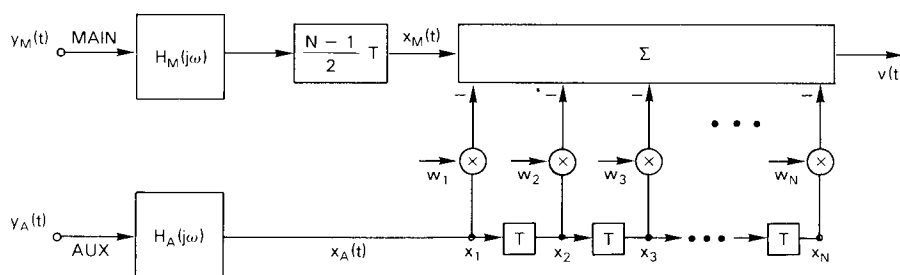


Fig. 1.1 — Two channel model of a compensated adaptive processor

To compensate for this mismatch, a transversal filter (or a tapped delay line) is inserted into the auxiliary channel, and weights $w_n, n = 1, 2, \dots, N$ on these taps are adjusted so that the output noise power residue of $v(t)$ (see Fig. 1.1) is minimized. Note that the time delay, T , normally approximates the Nyquist sampling interval: $1/B$ where B is the input signal's bandwidth. In addition, the main channel is delayed such that the auxiliary samples are time-centered.

If we define $\mathbf{w} = (w_1, w_2, \dots, w_N)^T$ to be the optimal complex valued weighting vector where T denotes the transpose operating, then it can be shown [1] that \mathbf{w} is the solution of the following vector equation:

$$\mathbf{R} \mathbf{w} = \mathbf{r} \quad (1.1)$$

where \mathbf{R} is the covariance matrix of the time delayed taps in the auxiliary channel and \mathbf{r} is the cross covariance vector between the auxiliary taps and the time-centered main channel. More formally

$$\mathbf{R} = E\{\mathbf{x}^* \mathbf{x}^T\} \quad (1.2)$$

and

$$\mathbf{r} = E\{\mathbf{x}^* x_M\} \quad (1.3)$$

where $E\{\cdot\}$ denotes the expected value, $*$ denotes the complex conjugate, and $\mathbf{x} = (x_1, x_2, \dots, x_N)^T$ is the vector of tapped time delayed signals in the auxiliary channels.

To completely understand the effects of the frequency mismatch errors, the statistical characteristics of the input signals must be known. However, in many instances this may not be possible. We have chosen to characterize and investigate the effects of the frequency mismatch errors on cancellation when the adaptive canceller is in the self-cancellation mode as illustrated in Fig 1.2. Here, we have tied the main and auxiliary inputs together and have inputted a wideband signal, $y(t)$. In this mode the optimal weights, \mathbf{w} , are chosen such that the product of $H_A(j\omega)$ and the transversal FTF match as closely as possible, $H_M(j\omega)$. We then calculate the output cancellation power residue. In a sense, the self-canceller mode yields best case (or an upper bound on) cancellation performance.

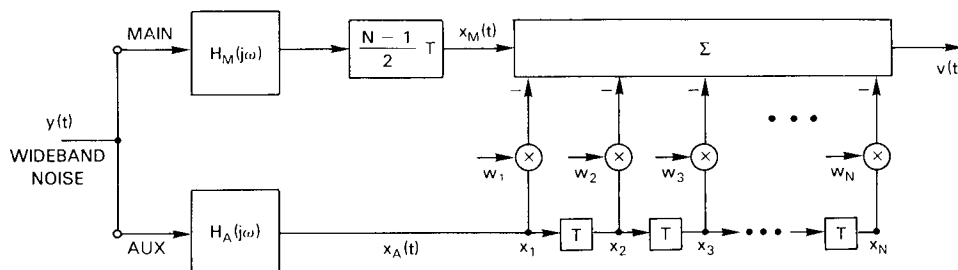


Fig. 1.2 — Self cancellation mode of a two channel compensated adaptive processor

This report is laid out as follows: Section II describes the pole/zero error model which is used to characterize the errors in filter fabrication. In Section III, a formula is derived for the output noise power residue of the self-canceller. In Section IV, a formulation is given for the special case of when the desired FTF is a Butterworth filter. Results generated from this analysis are presented in Section V.

II. POLE/ZERO ERROR MODEL

In this section, we develop a first order pole/zero error model for the frequency transfer functions (FTF) of the main and auxiliary channels: $H_M(j\omega)$ and $H_A(j\omega)$, respectively. This error model will allow us to derive a closed form solution for the cancellation residue as a function of the adaptive canceller system parameters. We assume that both these FTFs are designed to be some desired FTF: $H(j\omega)$. However, because of errors in the synthesis process, the poles and zeroes of $H(j\omega)$ will not be as designed and will have small perturbations around the desired poles and zeroes. This is illustrated in Fig. 2.1. These perturbations are assumed small enough so that we can use first order approximations for the filter responses in the main and auxiliary channels.

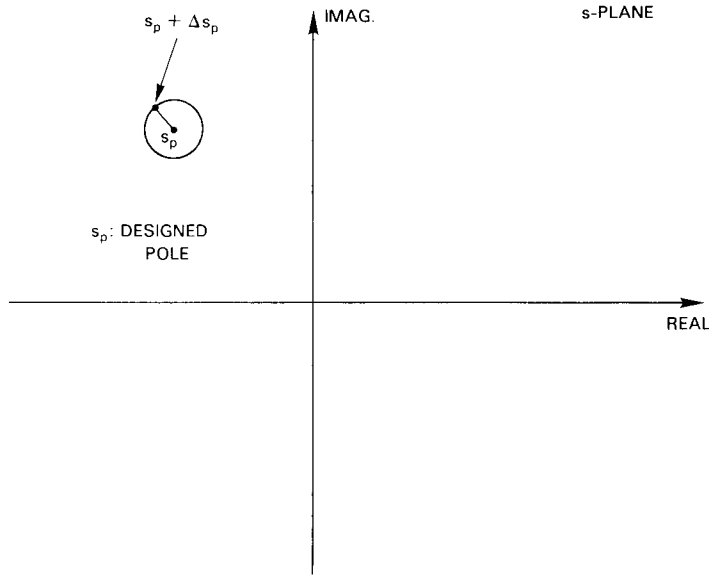


Fig. 2.1 — Pole with perturbation

We assume that real and imaginary parts of each perturbation are statistically independent and identically distributed zero mean random real variables. Also, for convenience we assume that the perturbations are statistically independent and identically distributed random complex variables. The variance of the magnitude of each perturbation is denoted by σ_F^2 . Later, we show that the identically distributed limitation can be deleted. We note at this time that this variance may be a function of the order of filter and moreover each perturbation of a pole or zero may have a different variance.

We assume that the desired FTF is a ratio of polynomials such that

$$H(j\omega) = \frac{P(j\omega)}{Q(j\omega)} \tag{2.1}$$

where $P(\cdot)$ and $Q(\cdot)$ are polynomials of order m and n , respectively. Consider the Laplace transform representations of $P(j\omega)$ and $Q(j\omega)$: $P(s)$ and $Q(s)$. Let $s_1^{(p)}, s_2^{(p)}, \dots, s_m^{(p)}$ be the roots of $P(s)$ and $s_1^{(q)}, s_2^{(q)}, \dots, s_n^{(q)}$ be the roots of $Q(s)$. Therefore $P(j\omega)$ and $Q(j\omega)$ can be expressed as

$$P(j\omega) = (j\omega - s_1^{(p)}) \dots (j\omega - s_m^{(p)}), \tag{2.2}$$

$$Q(j\omega) = (j\omega - s_1^{(q)}) \dots (j\omega - s_n^{(q)}). \tag{2.3}$$

Consider just $P(j\omega)$. Let each root, $s_k^{(p)}, k = 1, 2, \dots, m$ be perturbed by a small amount, $\Delta s_k^{(p)}$. Then the numerator polynomial is actually $\tilde{P}(j\omega)$, where

$$\tilde{P}(j\omega) = (j\omega - s_1^{(p)} - \Delta s_1^{(p)}) \dots (j\omega - s_m^{(p)} - \Delta s_m^{(p)}). \tag{2.4}$$

We assume that no roots of $P(s)$ and $Q(s)$ lie on or are arbitrarily close to the $j\omega$ axis. This assumption allows us to write an expansion of $\tilde{P}(j\omega)$ and $\tilde{Q}(j\omega)$ which does not have any singular points. If we expand Eq. (2.4) and retain only the lower order terms, then

$$\begin{aligned}
 \tilde{P}(j\omega) &= (j\omega - s_1^{(p)}) \dots (j\omega - s_m^{(p)}) \\
 &\quad - \sum_{k=1}^m (j\omega - s_1^{(p)}) \dots (j\omega - s_{k-1}^{(p)}) (j\omega - s_{k+1}^{(p)}) \dots (j\omega - s_m^{(p)}) \Delta s_k^{(p)} \\
 &= (j\omega - s_1^{(p)}) \dots (j\omega - s_m^{(p)}) \left[1 - \sum_{k=1}^m \frac{\Delta s_k^{(p)}}{j\omega - s_k^{(p)}} \right] \\
 &= P(j\omega) \left[1 - \sum_{k=1}^m \frac{\Delta s_k^{(p)}}{j\omega - s_k^{(p)}} \right].
 \end{aligned} \tag{2.5}$$

Similarly, we can show that the denominator polynomial when perturbed has the form

$$\tilde{Q}(j\omega) = Q(j\omega) \left[1 - \sum_{k=1}^n \frac{\Delta s_k^{(q)}}{j\omega - s_k^{(q)}} \right]. \tag{2.6}$$

Therefore, the perturbed FTF has the form

$$\tilde{H}(j\omega) = \frac{P(j\omega)}{Q(j\omega)} \cdot \frac{1 - \sum_{k=1}^m \frac{\Delta s_k^{(p)}}{j\omega - s_k^{(p)}}}{1 - \sum_{k=1}^n \frac{\Delta s_k^{(q)}}{j\omega - s_k^{(q)}}} \tag{2.7}$$

or

$$\tilde{H}(j\omega) = H(j\omega) \left[1 + \sum_{k=1}^n \frac{\Delta s_k^{(q)}}{j\omega - s_k^{(q)}} - \sum_{k=1}^m \frac{\Delta s_k^{(p)}}{j\omega - s_k^{(p)}} \right] \tag{2.8}$$

where we have retained only the lower order terms.

We rewrite Eq. (28) as

$$\tilde{H}(j\omega) = H(j\omega) \left[1 + \sum_{k=1}^{n+m} \frac{\Delta s_k}{j\omega - s_k} \right] \tag{2.9}$$

where we have set

$$\left. \begin{aligned} \Delta s_k &= \Delta s_k^{(p)} \\ s_k &= s_k^{(p)} \end{aligned} \right\} k = 1, 2, \dots, m \tag{2.10}$$

and

$$\left. \begin{aligned} \Delta s_{m+k} &= \Delta s_k^{(q)} \\ s_{m+k} &= s_k^{(q)} \end{aligned} \right\} k = 1, 2, \dots, n. \tag{2.11}$$

As it was previously mentioned, we assume that H_M and H_A are designed to be matched to $H(j\omega)$, but because of inaccuracies are not equal to $H(j\omega)$. We use the pole/zero error model to express

$$H_M(j\omega) = H(j\omega) \left[1 + \sum_{m=1}^M \frac{\Delta s_m^{(M)}}{j\omega - s_m} \right] \tag{2.12}$$

and

$$H_A(j\omega) = H(j\omega) \left[1 + \sum_{m=1}^M \frac{\Delta s_m^{(A)}}{j\omega - s_m} \right] \quad (2.13)$$

where M is the number of poles and zeros of $H(j\omega)$ and m is now an index. The parameters $s_m, m = 1, 2, \dots, M$ are some ordering of the poles and zeros of $H(j\omega)$, and $\Delta s_m^{(A)}, \Delta s_m^{(M)}$ are the perturbations of the poles and zeros of $H_A(j\omega)$ and $H_M(j\omega)$, respectively. These perturbations are assumed to be independent and identically distributed for both $H_A(j\omega)$ and $H_M(j\omega)$.

We set

$$\Delta H_A(j\omega) = \sum_{m=1}^M \frac{\Delta s_m^{(A)}}{j\omega - s_m} \quad (2.14)$$

and

$$\Delta H_M(j\omega) = \sum_{m=1}^M \frac{\Delta s_m^{(M)}}{j\omega - s_m}. \quad (2.15)$$

Therefore, the first order approximations of the perturbed main and auxiliary channel's FTF are

$$H_M(j\omega) = H(j\omega) (1 + \Delta H_M(j\omega)) \quad (2.16)$$

$$H_A(j\omega) = H(j\omega) (1 + \Delta H_A(j\omega)). \quad (2.17)$$

III. RESIDUE DERIVATION

In this section, we derive an expression for the output residue of the compensated canceller seen in Fig. 1.2. From this figure, we see that the output voltage, $v(t)$, can be expressed as

$$v(t) = x_M(t) - \mathbf{w}^T \mathbf{x}(t). \quad (3.1)$$

If we set

$$P_{\text{out}} = E\{|v(t)|^2\} \quad (3.2)$$

and

$$P_{\text{in}} = E\{|x_M(t)|^2\} \quad (3.3)$$

where P_{out} and P_{in} are the output and input noise powers, respectively, then we can show [1] that

$$P_{\text{out}} = P_{\text{in}} - \mathbf{w}' \mathbf{R} \mathbf{w} \quad (3.4)$$

where \mathbf{R} is defined by Eq. (1.2) and \mathbf{w} is the vector solution of Eq. (1.1). In fact, by using Eq. (1.1), we can show that

$$P_{\text{out}} = P_{\text{in}} - \mathbf{r}' \mathbf{R}^{-1} \mathbf{r} \quad (3.5)$$

where t denotes the complex conjugate transpose operation. The output cancellation (or noise attenuation factor) $P_{\text{out}}/P_{\text{in}}$ can then be expressed by

$$\frac{P_{\text{out}}}{P_{\text{in}}} = \frac{P_{\text{in}} - \mathbf{r}' \mathbf{R}^{-1} \mathbf{r}}{P_{\text{in}}}. \quad (3.6)$$

Note for the self-canceller that if $H_A(j\omega) = H_M(j\omega)$, that $P_{\text{out}}/P_{\text{in}} = 0$. We can show this as follows. Under the previous assumption of this analysis that the main and auxiliary inputs are identical, the optimal weighting, \mathbf{w}_0 , for the self canceller is

$$\begin{aligned} & \frac{N+1}{2} \text{ position} \\ & \quad \downarrow \\ \mathbf{w}_0 &= (0 \ 0 \ \dots \ 1 \ 0 \ 0 \ \dots \ 0)^T. \end{aligned} \quad (3.7)$$

This is due to the fact that

$$x_{N_2}(t) = x_M(t) \quad (3.8)$$

where we have set

$$N_2 = \frac{N+1}{2}. \quad (3.9)$$

Hence, we simply subtract the N_2 th output of the transversal filter seen in Fig. 1.2 from the output of the time delay element in the main channel to yield zero output noise power residue. As a result, if \mathbf{r}_0 and \mathbf{R}_0 are the cross covariance vector and covariance matrix under these ideal conditions (perfect matched filters), then

$$\begin{aligned} & \frac{N+1}{2} \text{ position} \\ & \quad \downarrow \\ \mathbf{R}_0^{-1}\mathbf{r}_0 &= \mathbf{w}_0 = (0 \ 0 \ \dots \ 1 \ 0 \ \dots \ 0)^T \end{aligned} \quad (3.10)$$

We use the result of Eq. (3.10) quite often in the upcoming derivations to simplify many of our expressions.

The noise power spectrum $S_{yy}(\omega)$, of $y(t)$ is assumed to be white so that $S_{yy}(\omega) = 1$ for all ω . Expressions for the elements of \mathbf{R}_0 and \mathbf{r}_0 are easily derivable. It can be shown that if $R_{0, nm}$ is the nm th element of the matrix \mathbf{R}_0 , then

$$R_{0, nm} = a \int_{-\infty}^{\infty} |H(j\omega)|^2 e^{j\omega\pi BT(n-m)} d\omega \quad n, m = 1, 2, \dots, N \quad (3.11)$$

where a is some nonzero proportionality constant. In fact, in the following discussions we arbitrarily set $a = 1$ because we will be dealing with ratios of powers which implies that none of the outputs calculated will be a function of a . Note that we have normalized the angular frequency to the desired angular bandwidth πB where B is the frequency bandwidth of the desired FTF, $H(j\omega)$. Similarly, if $r_{0, n}$ is the n th element of \mathbf{r}_0 , then

$$\mathbf{r}_{0, n} = \int_{-\infty}^{\infty} |H(j\omega)|^2 e^{j\omega\pi BT(n-N_2)} d\omega \quad n = 1, 2, \dots, N. \quad (3.12)$$

We define the elements of the inverse of \mathbf{R}_0 as

$$\mathbf{R}_0^{-1} = (R_0^{(nm)}) \quad n, m = 1, 2, \dots, N. \quad (3.13)$$

Expressions for the elements of \mathbf{R} and \mathbf{r} are given by

$$R_{nm} = \int_{-\infty}^{\infty} |H_A(j\omega)|^2 e^{j\omega\pi BT(n-m)} d\omega \quad n, m = 1, 2, \dots, N \quad (3.14)$$

and

$$r_n = \int_{-\infty}^{\infty} H_A^*(j\omega) H_M(j\omega) e^{j\omega\pi BT(n-N_2)} d\omega \quad n = 1, 2, \dots, N. \quad (3.15)$$

If we use the first order approximations of $H_M(j\omega)$ and $H_A(j\omega)$ given by Eqs. (2.16) and (2.17) respectively, we can show by using Eqs. (3.14) and (3.15) that

$$R_{nm} = R_{0,nm} + \Delta R_{nm} \quad n, m = 1, 2, \dots, N \quad (3.16)$$

$$r_n = r_{0,n} + \Delta r_n \quad n = 1, 2, \dots, N \quad (3.17)$$

where

$$\Delta R_{nm} = \int_{-\infty}^{\infty} |H|^2 (\Delta H_A + \Delta H_A^*) e^{j\omega\pi BT(n-m)} d\omega + \int_{-\infty}^{\infty} |H|^2 |\Delta H_A|^2 e^{j\omega\pi BT(n-m)} d\omega \quad n, m = 1, 2, \dots, N \quad (3.18)$$

and

$$\Delta r_n = \int_{-\infty}^{\infty} |H|^2 (\Delta H_A^* + \Delta H_M^*) e^{j\omega\pi BT(n-N_2)} d\omega + O(\Delta H_A^* \Delta H_M) \quad n = 1, 2, \dots, N. \quad (3.19)$$

Furthermore, if we define

$$P_{in} = P_{in}^{(0)} + \Delta P_{in} \quad (3.20)$$

where $P_{in}^{(0)}$ is the input power when there are no perturbations, then we can show that

$$\Delta P_{in} = \int_{-\infty}^{\infty} |H|^2 (\Delta H_M + \Delta H_M^*) d\omega + \int_{-\infty}^{\infty} |H|^2 |\Delta H_M|^2 d\omega. \quad (3.21)$$

We rewrite the output power residue given by Eq. (3.5) in terms of the perturbations given by Eqs. (3.16), (3.17), and (3.20):

$$P_{out} = P_{in}^{(0)} + \Delta P_{in} - (\mathbf{r}_0 + \Delta \mathbf{r})' (\mathbf{R}_0 + \Delta \mathbf{R})^{-1} (\mathbf{r}_0 + \Delta \mathbf{r}) \quad (3.22)$$

where

$$\Delta \mathbf{r} = (\Delta r_1, \Delta r_2, \dots, \Delta r_N)^T \quad (3.23)$$

and

$$\Delta \mathbf{R} = (\Delta R_{nm}) \quad n, m = 1, 2, \dots, N. \quad (3.24)$$

Note that the $\Delta \mathbf{R}$ matrix is hermitian Toeplitz. We use a second order approximation of $(\mathbf{R}_0 + \Delta \mathbf{R})^{-1}$. This can be shown to be

$$(\mathbf{R}_0 + \Delta \mathbf{R})^{-1} = \mathbf{R}_0^{-1} - \mathbf{R}_0^{-1} \Delta \mathbf{R} \mathbf{R}_0^{-1} + \mathbf{R}_0^{-1} \Delta \mathbf{R} \mathbf{R}_0^{-1} \Delta \mathbf{R} \mathbf{R}_0^{-1}. \quad (3.25)$$

If Eq. (3.22) is expanded and only the second order and below perturbation terms are retained, then

$$\begin{aligned} P_{out} = & P_{in}^{(0)} + \Delta P_{in} - \mathbf{r}_0' \mathbf{R}_0^{-1} \mathbf{r}_0 - \Delta \mathbf{r}' \mathbf{R}_0^{-1} \mathbf{r}_0 - \mathbf{r}_0' \mathbf{R}_0^{-1} \Delta \mathbf{r} \\ & - \Delta \mathbf{r}' \mathbf{R}_0^{-1} \Delta \mathbf{r} + \mathbf{r}_0' \mathbf{R}_0^{-1} \Delta \mathbf{R} \mathbf{R}_0^{-1} \mathbf{r}_0 + \Delta \mathbf{r}' \mathbf{R}_0^{-1} \Delta \mathbf{R} \mathbf{R}_0^{-1} \mathbf{r}_0 \\ & + \mathbf{r}_0' \mathbf{R}_0^{-1} \Delta \mathbf{R} \mathbf{R}_0^{-1} \Delta \mathbf{r} - \mathbf{r}_0' \mathbf{R}_0^{-1} \Delta \mathbf{R} \mathbf{R}_0^{-1} \Delta \mathbf{R} \mathbf{R}_0^{-1} \mathbf{r}_0. \end{aligned} \quad (3.26)$$

Note that an immediate simplification of Eq. (3.26) results because

$$P_{in}^{(0)} - \mathbf{r}_0' \mathbf{R}_0^{-1} \mathbf{r}_0 = 0. \quad (3.27)$$

We average P_{out} over the identical zero mean probability density functions (p.d.f.'s) of the pole and zero perturbations in order to obtain an average cancellation residue. Since the p.d.f.'s are zero mean, it follows immediately that

$$E\{\Delta \mathbf{r}' \mathbf{R}_0^{-1} \mathbf{r}_0\} = 0 \quad (3.28)$$

and

$$E\{\mathbf{r}_0 \mathbf{R}_0^{-1} \Delta \mathbf{r}\} = 0. \quad (3.29)$$

Further simplifications are possible due to Eq. (3.10). Derivations of the rest of the terms in Eq. (3.26) averaged over the pole/zero perturbations are given in Appendix A. We merely state the results. If σ_F^2 is the variance of a pole/zero perturbation, then

$$E\{\Delta P_{\text{in}}\} = \sigma_F^2 \Gamma_1 \quad (3.30)$$

$$E\{\Delta \mathbf{r}' \mathbf{R}_0^{-1} \Delta \mathbf{r}\} = 2\sigma_F^2 \Gamma_2 \quad (3.31)$$

$$E\{\mathbf{r}_0 \mathbf{R}_0^{-1} \Delta \mathbf{R} \mathbf{R}_0^{-1} \Delta \mathbf{R}\} = E\{\Delta \mathbf{r}' \mathbf{R}_0^{-1} \Delta \mathbf{R} \mathbf{R}_0^{-1} \mathbf{r}_0\} = \sigma_F^2 \Gamma_2 \quad (3.32)$$

$$E\{\mathbf{r}_0 \mathbf{R}_0^{-1} \Delta \mathbf{R} \mathbf{R}_0^{-1} \mathbf{r}_0\} = \sigma_F^2 \Gamma_1 \quad (3.33)$$

$$E\{\mathbf{r}_0 \mathbf{R}_0^{-1} \Delta \mathbf{R} \mathbf{R}_0^{-1} \Delta \mathbf{R} \mathbf{R}_0^{-1} \mathbf{r}_0\} = 2\sigma_F^2 \Gamma_2 \quad (3.34)$$

where

$$\Gamma_1 = \sum_{i=1}^M \int_{-\infty}^{\infty} \frac{|H|^2 d\omega}{|j\omega - s_i|^2} \quad (3.35)$$

and

$$\Gamma_2 = \sum_{i=1}^M \sum_{k=1}^N \sum_{m=1}^N \left[R_0^{(km)} \cdot \int_{-\infty}^{\infty} \frac{|H|^2 e^{j\omega\pi BT(N_2-k)} d\omega}{j\omega - s_i} \cdot \int_{-\infty}^{\infty} \frac{|H|^2 e^{j\omega\pi BT(m-N_2)} d\omega}{-j\omega - s_i^*} \right]. \quad (3.36)$$

We define $P_{\text{out}}^{(\text{ave})}$ to be equal to P_{out} average over all the perturbations. Examining Eq. (3.6) and Eqs. (3.30) to (3.34), we see by use of the above results that $P_{\text{out}}^{(\text{ave})}/P_{\text{in}}$ is proportional to σ_F^2 and that the constant of proportionality in the first order approximation does not change if we set $P_{\text{in}} = P_{\text{in}}^{(0)}$. By adjusting the gain of $|H(j\omega)|^2$ we can arbitrarily set $P_{\text{in}}^{(0)} = 1$; i.e.,

$$\int_{-\infty}^{\infty} |H(j\omega)|^2 d\omega = 1. \quad (3.37)$$

Thus by substituting Eqs. (3.30) to (3.36) into Eq. (3.26), and by simplifying and normalizing we can show that

$$\frac{P_{\text{out}}^{(\text{ave})}/P_{\text{in}}}{\sigma_F^2} = 2 \sum_{i=1}^M \left[\int_{-\infty}^{\infty} \frac{|H|^2 d\omega}{|j\omega - s_i|^2} - \sum_{k=1}^N \sum_{m=1}^N R_0^{(km)} \int_{-\infty}^{\infty} \frac{|H|^2 e^{j\omega\pi BT(N_2-k)} d\omega}{j\omega - s_i} \cdot \int_{-\infty}^{\infty} \frac{|H|^2 e^{j\omega\pi BT(m-N_2)} d\omega}{-j\omega - s_i^*} \right]. \quad (3.38)$$

We call $[P_{\text{out}}^{(\text{ave})}/P_{\text{in}}]/\sigma_F^2$ the cancellation-filter mismatch ratio, CFMR.

We note that the restriction that all the poles and zeroes have the same variance, σ_F^2 , can be easily removed. If $\sigma_{F_m}^2$ is the variance of the perturbation on the m th pole or zero of $H(s)$, then we

could have simply expanded $P_{\text{out}}^{(\text{ave})}$ in terms of $\sigma_{F_m}^2$, $m = 1, 2, \dots, M$. The resultant formulation would have exactly the same form as Eq. (3.38) except that σ_F^2 is replaced by $\sigma_{F_{\text{ave}}}^2$ where

$$\sigma_{F_{\text{ave}}}^2 = \frac{1}{M} \sum_{m=1}^M \sigma_{F_m}^2. \quad (3.39)$$

IV. A SPECIAL CASE: THE BUTTERWORTH FILTER

In this section we evaluate the cancellation-filter mismatch ratio, CFMR, for the case when the desired transfer function is a Butterworth filter. This filter is of much interest because it is easily synthesized and is a bandpass filter with the attenuation of the skirts controlled by the order of the filter.

This filter has the following magnitude squared angular frequency response:

$$|H(j\omega)|^2 = \frac{c_0}{1 + \omega^{2M}} \quad (4.1)$$

where M defines the order of the filter, the angular frequency has been normalized to the desired angular bandwidth, πB , and

$$c_0 = \frac{M}{\pi} \sin \frac{\pi}{2M}. \quad (4.2)$$

The constant c_0 has been chosen so that Eq. (3.37) is satisfied. Curves of the Butterworth filter response are shown in Fig. 4.1 for various values of M . Note, that by increasing the order of the Butterworth filter, M , that the skirts of the bandpass filter become more attenuated.

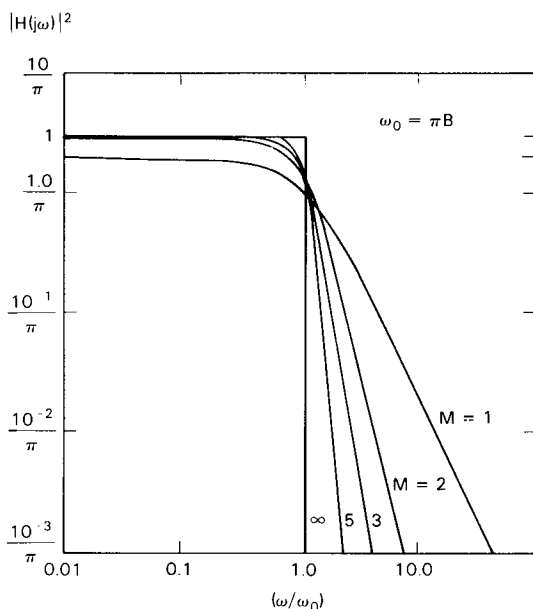


Fig. 4.1 — Butterworth filter response

The filter is synthesized by finding an $H(s)$ function whose poles are in the left-hand side of the s -plane such that

$$H(s)H(-s)|_{s=j\omega} = |H(j\omega)|^2. \quad (4.3)$$

Now the poles of $|H(j\omega)|^2$ can be shown to lie on the unit circle and are spaced equally in angle as illustrated in Fig. 4.2 for $M = 3$. Hence in order to find $H(s)$, the M left-hand plane poles of $|H(j\omega)|^2$ are identified and used to form the polynomial, $H(s)$; i.e., if s_i , $i = 1, 2, \dots, M$ are the left-handed poles, then

$$H(s) = \sqrt{c_0}[(s - s_1)(s - s_2) \dots (s - s_M)]^{-1}. \quad (4.4)$$

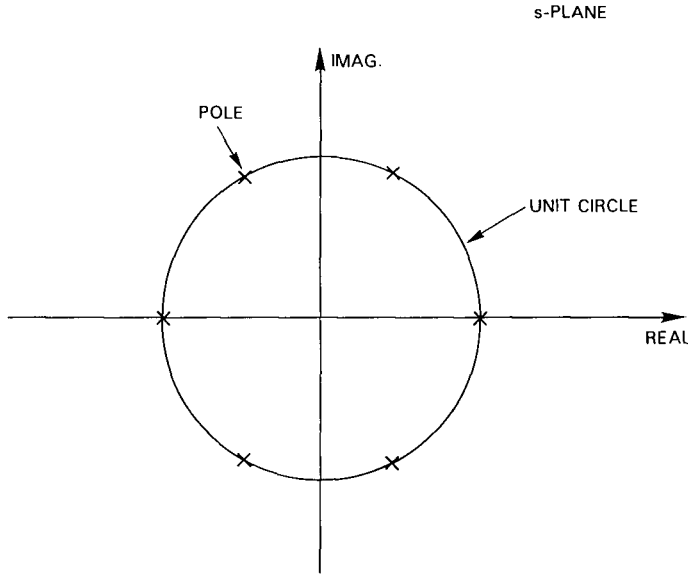


Fig. 4.2 — Pole plot of Butterworth filter of order, 3

To evaluate the CFMR, the integrals of Eqs. (3.35) and (3.36) must be evaluated. This can be done by using the Theory of Residues [2] and is outlined in Appendix B where expressions for these integrals are obtained. From Eq. (3.38), we also need an exact expression for the elements of \mathbf{R}_0 from which the elements of \mathbf{R}_0^{-1} can be obtained through matrix inversion. Summarizing the results of Appendix B:

$$R_{nm} = \frac{\pi c_0}{M} \sum_{l=1}^M e^{\pi BT(n-m)\sin\frac{\pi}{2M}(2l-1)} e^{j\pi\left(\frac{1}{2}-\frac{1}{2M}(2l-1)+BT(n-m)\cos\frac{\pi}{2M}(2l-1)\right)} \quad \text{for } m > n \quad (4.5a)$$

$$R_{nm} = \frac{\pi c_0}{M} \sum_{l=1}^M e^{-\pi BT(n-m)\sin\frac{\pi}{2M}(2l-1)} e^{j\pi\left(-\frac{1}{2}+\frac{1}{2M}(2l+1)+BT(n-m)\cos\frac{\pi}{2M}(2l-1)\right)} \quad \text{for } m \leq n \quad (4.5b)$$

$$\int_{-\infty}^{\infty} \frac{|H|^2 d\omega}{|j\omega - s_i|^2} = \frac{\pi c_0}{2} \frac{1}{\sin\frac{\pi}{2M}(2i-1)} \quad (4.6)$$

$$\begin{aligned} & \int_{-\infty}^{\infty} \frac{|H|^2 e^{j\omega\pi BT(N_2-n)}}{j\omega - s_i} d\omega \\ &= \frac{\pi c_0}{M} \sum_{m=1}^M \frac{e^{(N_2-n)\pi BT\sin\frac{\pi}{2M}(2m-1)} e^{j(N_2-n)\pi BT\cos\frac{\pi}{2M}(2m-1)}}{1 - e^{j\frac{\pi}{M}(i+m-1)}} \quad \text{for } N_2 \leq n \end{aligned} \quad (4.7a)$$

$$\int_{-\infty}^{\infty} \frac{|H|^2 e^{j\omega \pi BT (N_2 - n)}}{j\omega - s_i} d\omega$$

$$= \frac{\pi c_0}{M} \sum_{m=1}^M \left[(M - .5 - (N_2 - n) \pi BT j e^{j \frac{\pi}{2M} (2i-1)}) \delta_{im} - \frac{1 - \delta_{im}}{1 - e^{j \frac{\pi}{M} (i-m)}} \right]$$

$$\cdot e^{-\frac{(N_2 - n) \pi BT \sin \frac{\pi}{2M} (2m-1)}{j(N_2 - n) \pi BT \cos \frac{\pi}{2M} (2m-1)}} \quad \text{for } N_2 > n \quad (4.7b)$$

and

$$\int_{-\infty}^{\infty} \frac{|H|^2 e^{j\omega \pi BT (n - N_2)}}{-j\omega - s_i^*} d\omega = \left[\int_{-\infty}^{\infty} \frac{|H|^2 e^{j\omega \pi BT (N_2 - n)}}{j\omega - s_i} d\omega \right]^* \quad (4.8)$$

where

$$\delta_{im} = \begin{cases} 1 & \text{if } i = m \\ 0 & \text{otherwise} \end{cases} \quad (4.9)$$

Note that Eq. (4.8) follows by the definition of the complex conjugate operation.

V. RESULTS

A. Introduction

In this section, we present some results of the effects of frequency mismatch errors on self-cancellation. Specifically, curves of the Cancellation-Frequency Mismatch Ratio, CFMR, versus the various input parameters,

- M , the order of the Butterworth filter
- N , the number of time delay taps, and
- BT , the filter bandwidth-tapped time delay product

are plotted and discussed. Also, a procedure for choosing the "optimum" M , N , and BT is outlined in the Discussion subsection.

Note that in some cases the numerical calculations involved in obtaining CFMR were very sensitive to the eigenvalues of \mathbf{R}_0 , the ideal covariance matrix (even using double precision complex arithmetic on a VAX-750). Because of this sensitivity it was necessary to add statistically independent internal noise to each of the tapped delay outputs. In regards to \mathbf{R}_0 , this added an internal noise power term, σ_n^2 , to each of the diagonal elements of \mathbf{R}_0 . It was found that an external jamming (the self-cancellation input signal) to internal noise ratio, J/N , of 50 dB resulted in excellent numerical stability in calculating CFMR. Furthermore, if J/N were increased to 70 dB, the results changed minutely. Hence for the curves to be presented, we list the J/N under which the CFMR was calculated.

B. The Butterworth Filter Order

Figures 5.1 through 5.10 present plots of CFMR versus the order of the Butterworth filter, M . For each figure, BT is held constant and contours of CFMR with N , the number of time delay taps are plotted. We note that cancellation improves as CFMR decreases. From these figures, we observe that

- cancellation (or CFMR) obviously improves by increasing the number of time delay taps;
- the CFMR in many cases has a minimum as a function of the order of the Butterworth filter, M ; and
- the minimum also depends on the bandwidth-tapped time delay product, BT .

We discuss the first and third observations in more detail in subsections D and C, respectively.

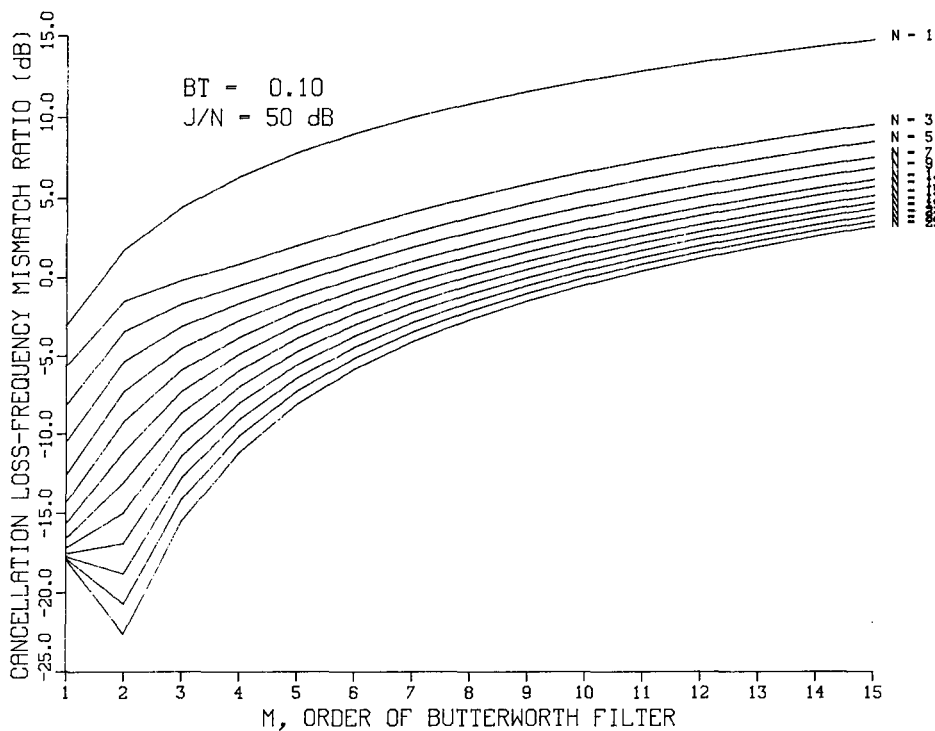


Fig. 5.1 — CFMR vs M , $BT = .1$

The occasional minimum in the curves as function of M can be explained as follows. There is a certain amount of aliasing which occurs due to the transversal filter in the auxiliary channel; i.e., the transversal filter has a periodic frequency response. Hence the tails of the main channel's perturbed Butterworth filter frequency response near the sampling rate frequency (which is assumed constant for each figure and related to BT) are not accurately matched. As the order of the Butterworth filter increases, these tails decrease in magnitude about the sampling rate frequency and hence auxiliary channel aliasing effects decrease. As a result there is better matching up to a point. The fact that we are degrees of freedom (DOF) limited (recall that N is assumed a constant), results in the CFMR increasing after reaching some minimum; i.e., the more poles in the Butterworth filter, the more irregularities in the frequency response which must be matched.

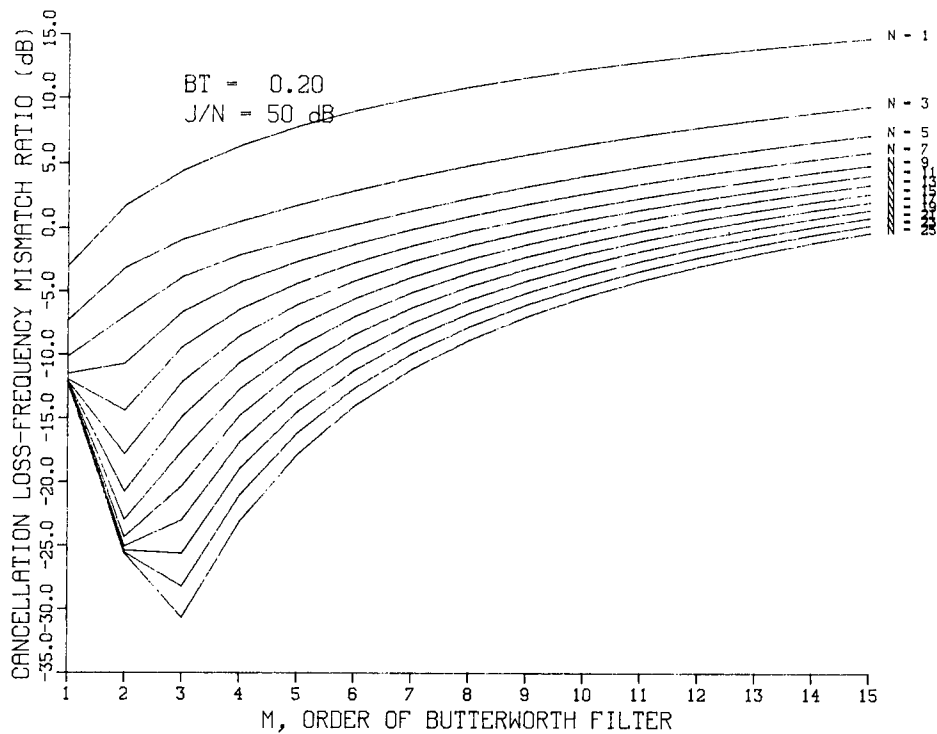


Fig. 5.2 - CFMR vs M , $BT = .2$

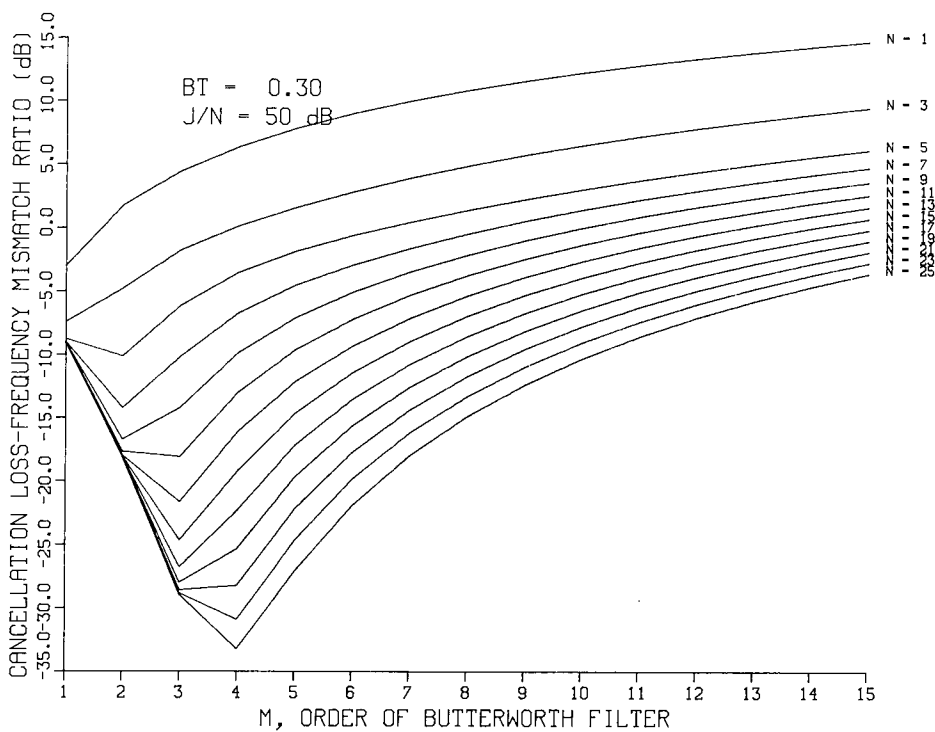


Fig. 5.3 - CFMR vs M , $BT = .3$

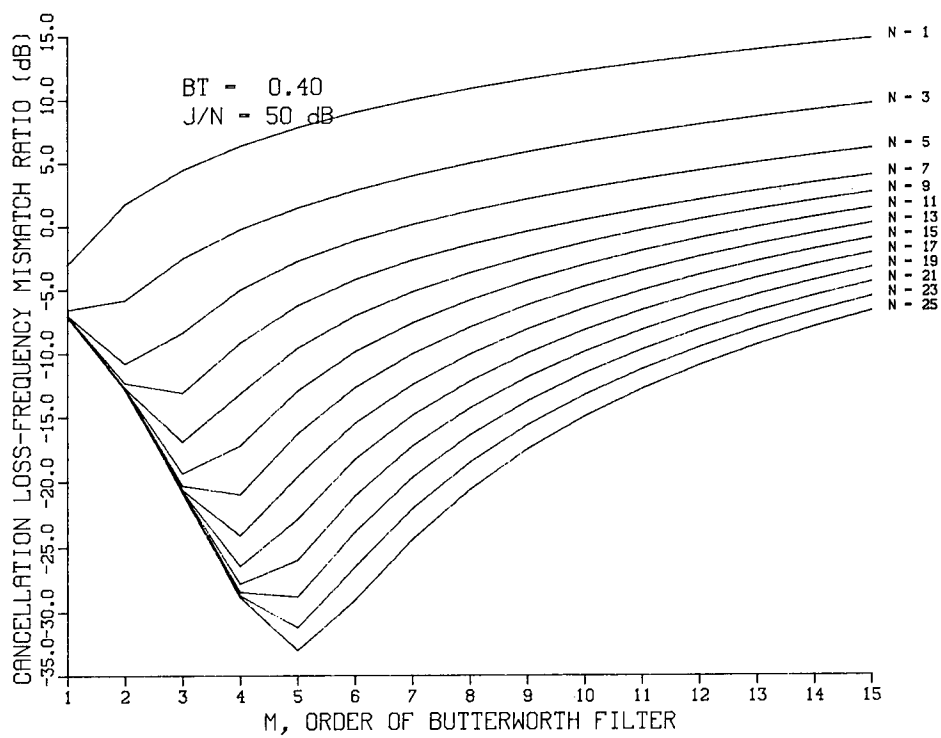


Fig. 5.4 - CFMR vs M , $BT = .4$

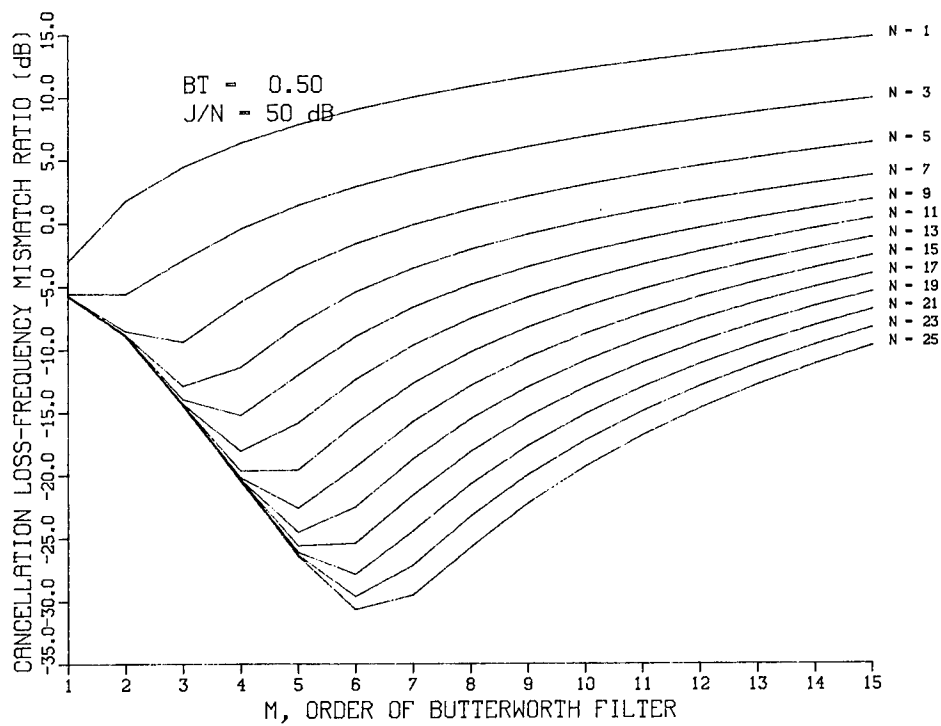


Fig. 5.5 - CFMR vs M , $BT = .5$

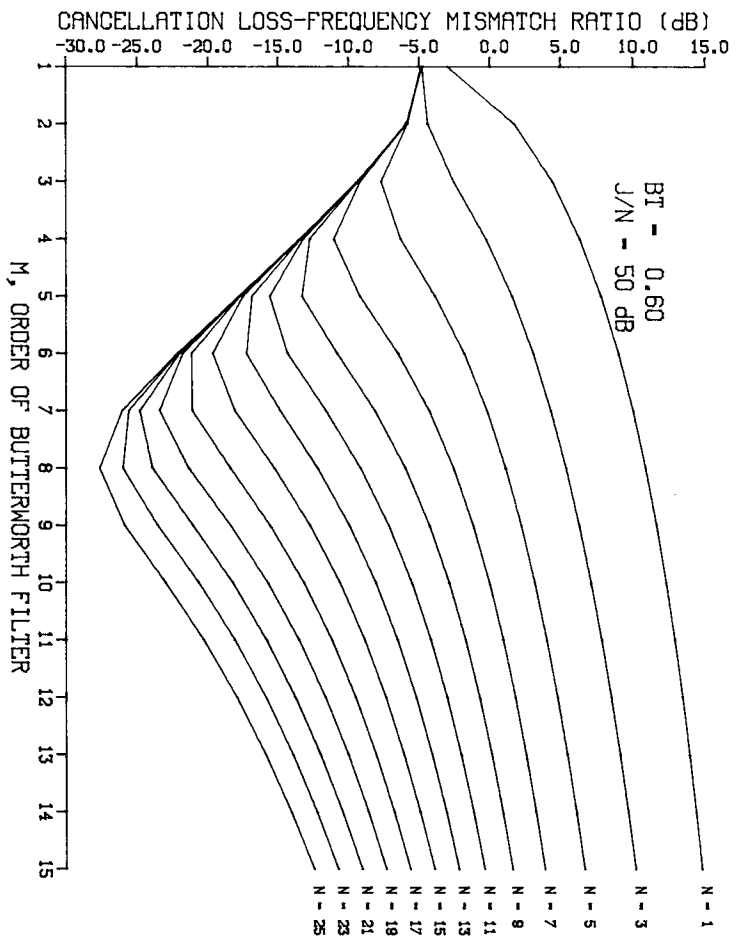


Fig. 5.6 - CFMR vs M, BT = .6

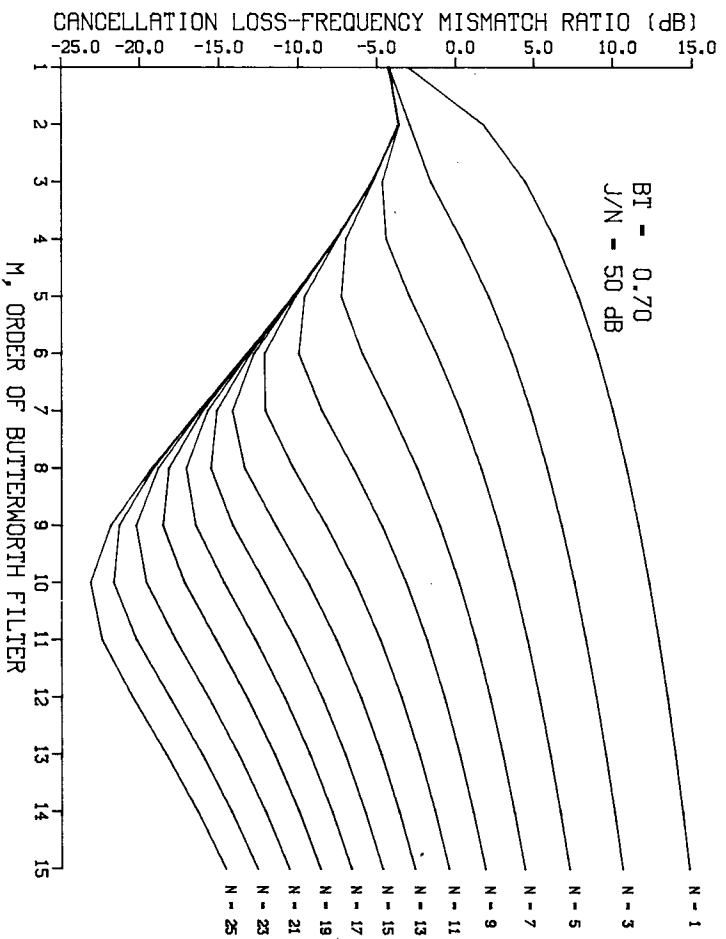


Fig. 5.7 - CFMR vs M, BT = .7

KARL GERLACH

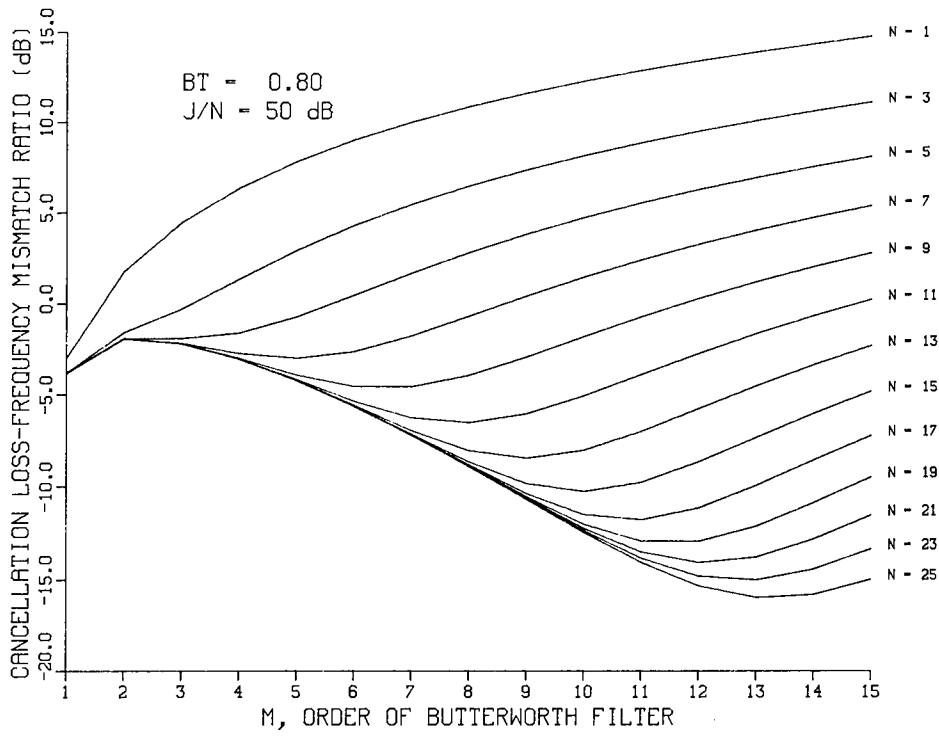


Fig. 5.8 - CFMR vs M, BT = .8

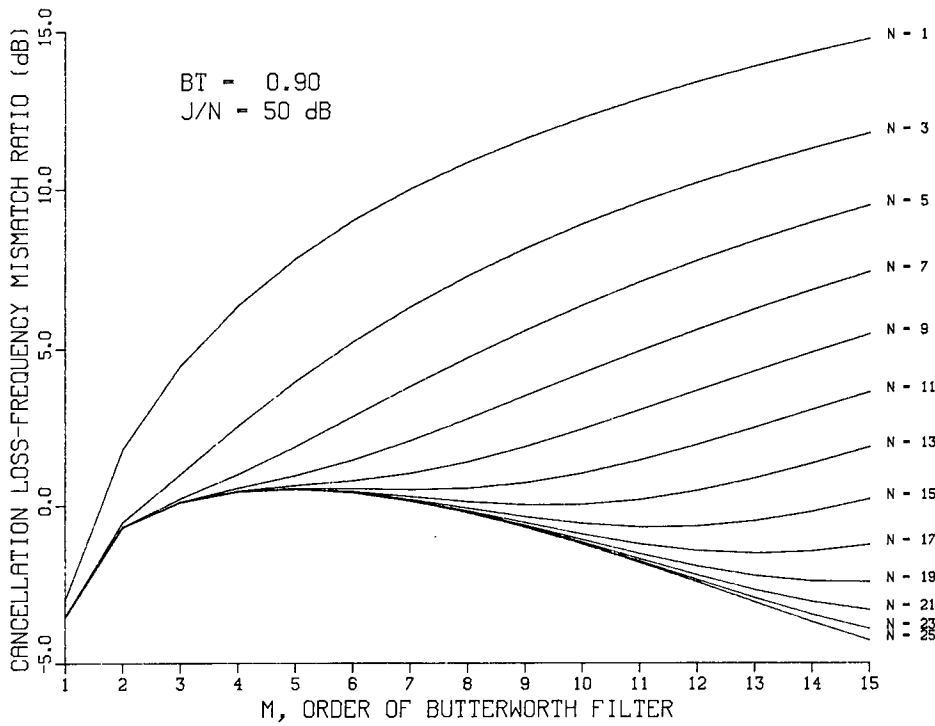
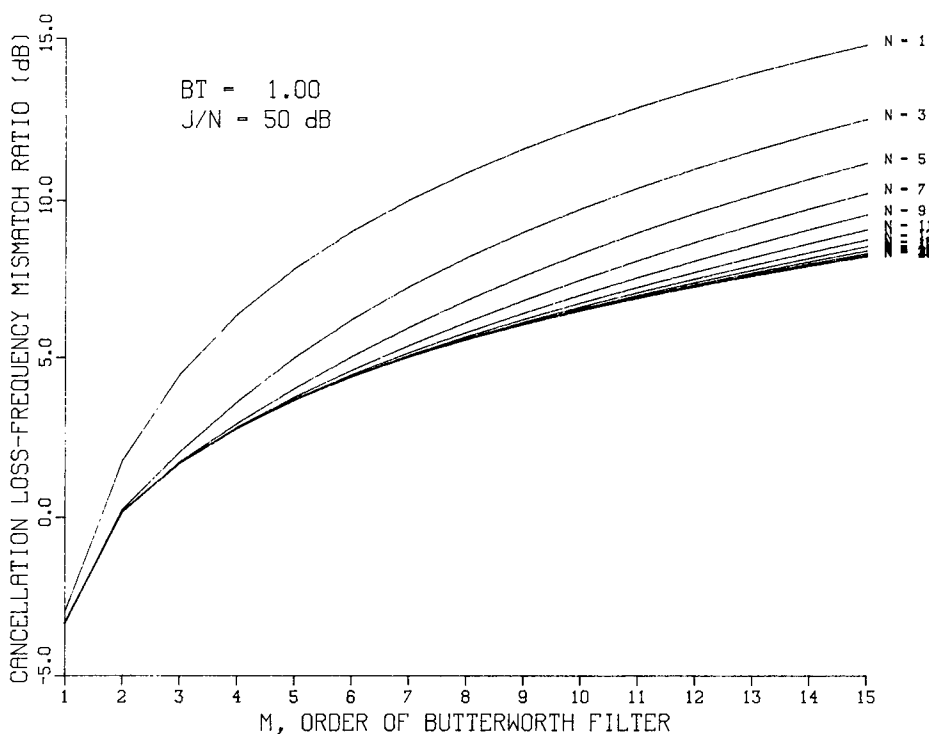


Fig. 5.9 - CFMR vs M, BT = .9

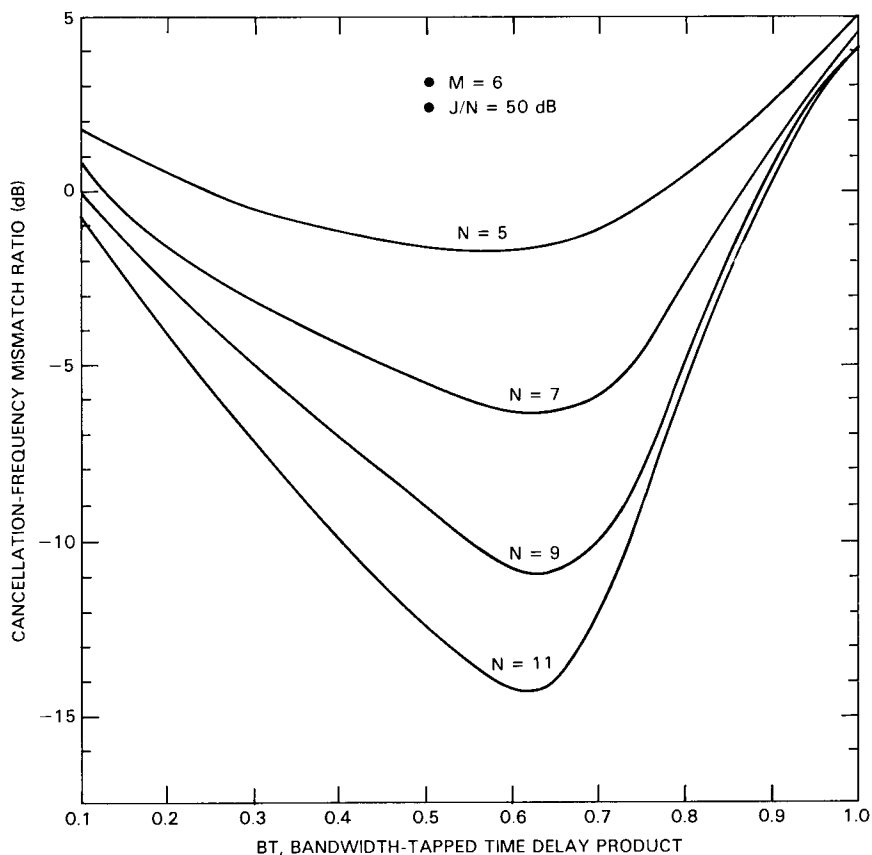
Fig. 5.10 — CFMR vs M , $BT = 1$

C. The Bandwidth-Tapped Time Delay Product

The minimum values of CFMR as seen in Figs. 5.1 to 5.9 are also functions of the bandwidth-tapped time delay product, BT . From these figures, we see that for a constant N and decreasing BT , that the minimal CFMR occurs at decreasing values of M . This can again be explained by considering aliasing effects: a higher sampling rate (or smaller BT) can tolerate a lower order of Butterworth filter while maintaining a constant aliasing degradation.

Note that by comparing Fig. 5.10 where $BT=1$ with Figs. 5.1 to 5.9 where $BT<1$, that sampling at the filter bandwidth (or the information bandwidth) results in very poor cancellation performance. This is again due to aliasing, which is caused by the periodic frequency response of the compensating transversal filter. Hence, for cancellation systems using a bandpass filter, one should never sample at the Nyquist rate if possible.

In Fig. 5.11, we have plotted CFMR versus BT for various values of N and $M = 6$. Here, we observe that the CFMR has a minimum with respect to BT (for this example, the minimums over all curves occurs when $BT \approx 0.6$). The value of CFMR decreases as BT decreases from one because the negative effects of aliasing are being reduced. However, as BT becomes smaller, the tapped time delay decreases and because there is a fixed number of taps, the transversal filter cannot accurately match the main channel's irregularities. In essence, the tails of the time correlation function associated with the power spectrum of the transversal filter degrades in matching the tails of the main channel's time correlation function (associated with its spectrum) because NT decreases as BT decreases. In the limit of course as BT or $T \rightarrow 0$, the transversal filter with N taps is equivalent to a transversal filter with just one tap (and no time delays). Hence, CFMR must increase as BT becomes very small.

Fig. 5.11 — CFMR vs BT , $M = 6$

D. The Number of Time Delay Taps

In Fig. 5.12, curves of CFMR are plotted versus N , the number of time delay taps for various values of M with $BT = 1$. It was previously observed that CFMR decreases as N increases for a constant M and BT . However, note that the cancellation goes to some lower bound as $N \rightarrow \infty$. This results because of the adaptive transversal filter, regardless of its order, is not a good match to the main channel beyond the sampling rate frequency. The main channel's frequency spectrum has tails which extend beyond the sampling rate frequency. These tails are poorly matched by the transversal filter, and a finite noise power residue results which is independent of N but dependent on BT and M . Hence, we see that merely increasing the number of time taps does *not* result in the cancelled noise residue going to zero or some arbitrarily small number. We also note that the CFMR is not necessarily monotonic with the order of the Butterworth filter, M , as depicted in Fig. 5.12 for when $BT = 1$. In fact for all cases, $BT < 1$, it is not.

E. Discussion

In this subsection, we briefly outline a design procedure for choosing BT , M , and N such that the cancellation is "optimized" in some sense. In our previous analysis, we have only considered one auxiliary channel. In many applications there are multiple auxiliary channels which are used to cancel the noise in the main channel. Each of these channels has a bandpass filter and an adaptive compensating transversal filter, as was shown for the case of the single auxiliary as seen in Fig. 1.1. For the self-canceller, because the adaptive transversal filter in each auxiliary channel attempts to match each of the

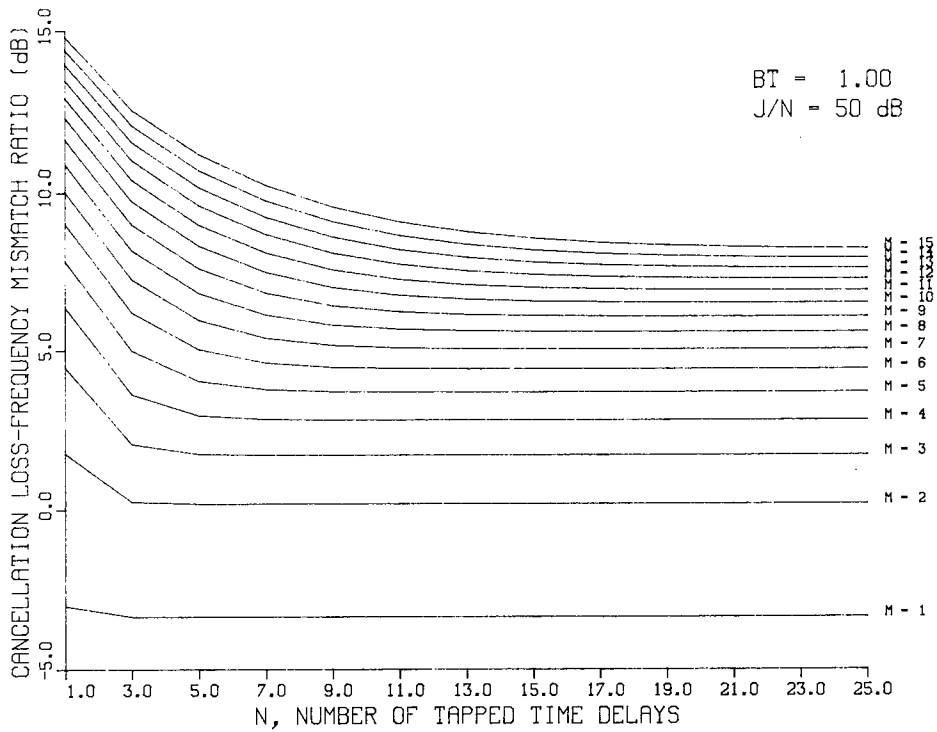


Fig. 5.12 — CFMR vs N , $BT = 1$

auxiliary channels to the main channel, we see that choosing the best BT , M , and N for one auxiliary channel is essentially equivalent to choosing the best BT , M , and N for any number of auxiliary channels. Hence, the design procedure, which will be outlined, is applicable to a canceller with any number of auxiliary channels.

Let us set

$$\frac{C}{\sigma_F^2} = \text{CFMR} \tag{5.1}$$

where

$$C = \frac{P_{\text{out}}^{(\text{ave})}}{P_{\text{in}}} \tag{5.2}$$

Here we have defined C to be the average cancellation. We can readily discern two types of optimization problems:

1. maximize (in a negative sense) the cancellation, C , under a given set of constraints or,
2. given a required C , maximize σ_F^2 under a given set of constraints.

For many kinds of antijamming design problems, the second type of problem is more realistic. In this case, we calculate how much cancellation is needed in a given jamming scenario, and try to relax to system specification, σ_F^2 , as much as possible.

Both types of design problems are subject to a number of constraints on M , N , and BT . We briefly list the constraints and some of the causes of these constraints.

- $N_{\min} \leq N$: set by the matching requirements among channels for the external signals, multipath, antennas, RF front ends, etc.
- $N \leq N_{\max}$: set by computational load limits, finite sampling window
- $BT_{\min} \leq BT$: information bandwidth requirement
- $BT \leq BT_{\max}$: system limitations
- $M \leq M_{\max}$: synthesis limitations, cost, response time
- $\sigma_{\bar{f}}^2 = f(M)$: error is a function of Butterworth filter order.

Note in the optimizations procedure for most cases the optimal N will equal N_{\max} . The last item mentioned above would have to be determined by a statistical analysis of the rms error of the poles as a function of the Butterworth filter order and the errors in the synthesis process.

Hence we see that given that the constraints on BT , M , and N are defined, and given the curves of CFMR (or Eq. 3.38), a computer search program could be developed which finds the BT , M , and N which either maximizes the cancellation (problem 1) or maximizes $\sigma_{\bar{f}}^2$ (problem 2, given C required).

We should point out, however, that one rarely goes to a filter designer with a specification such as the variance of the pole perturbation. Normally one specifies the ripple across the passband and the rms difference between the synthesized filter and the ideal filter across the passband. Hence the canceller designer must make a conversion from $\sigma_{\bar{f}}^2$ to these filter design parameters if some meaningful specification is to be made. After the filter is fabricated, the canceller designer can have the filter designer test the filter and see that the poles fall within the variance, $\sigma_{\bar{f}}^2$. (Note that if one specifies $\sigma_{\bar{f}_{\text{ave}}}^2$ over all poles to less than $\sigma_{\bar{f}}^2$, the filter specifications are satisfied.)

For example, let us assume that $\sigma_{\bar{f}}^2$ is not a function of M and that BT , M , and N have the following constraints: $1 \leq BT \leq 1$, $5 \leq N \leq 11$, $1 \leq M \leq 15$. We desire -30 dB of cancellation. Under these conditions, we would find that the optimal parameters are $BT = 0.4$, $N = 11$, and $M = 4$ with $\text{CFMR}_{\text{opt}} = -19$ dB. Hence $\sigma_{\bar{f}}^2 = -11$ dB, or the relative rms perturbation error on the poles is approximately 30%. Note that if we desired 50 dB of cancellation, this relative rms error would be approximately 3%.

VI. SUMMARY AND CONCLUSIONS

The effects of frequency mismatch errors on adaptive cancellers have been investigated. The frequency mismatch errors occur because of errors in the synthesis process of supposedly identical bandpass filters which are in each of the input channels. These frequency mismatches among the channels result in cancellation degradation. Tapped delay line transversal filters can be used to compensate for these frequency mismatches and thus improve cancellation performance.

A pole/zero error model of the filters has been developed whereby closed form solutions of the maximum achievable cancellation are obtained. This cancellation is a function of the order of the ideally matched frequency filters, the number of time delay taps in the compensating transversal filter, the bandwidth-tapped time delay product, and the constraints on these parameters. A design procedure was outlined for "optimizing" the canceller with respect to these parameters and their constraints. Specifically, results were presented for when the input filters are the Butterworth type. It was shown that an arbitrarily low output noise residue *cannot* be achieved by arbitrarily increasing the number of time delay taps.

VII. REFERENCES

1. R.A. Monzingo and T.W. Miller, *Introduction to Adaptive Arrays* (John Wiley and Sons, 1980).
2. R.V. Churchill, *Complex Variables and Applications* (McGraw-Hill, 1960).

Appendix A
DERIVATION OF EQUATIONS (3.30) TO (3.34)

1. *The $E\{\Delta P_{in}\}$ Term:*

We showed in the text (see Eq. 3.21) that

$$\Delta P_{in} = \int_{-\infty}^{\infty} |H|^2 (\Delta H_M + \Delta H_M^*) d\omega + \int_{-\infty}^{\infty} |H|^2 |\Delta H_M|^2 d\omega. \quad (A1)$$

Now

$$\Delta H_M(j\omega) = \sum_{i=1}^M \frac{\Delta s_i^{(M)}}{j\omega - s_i}. \quad (A2)$$

Let $\Delta s_i^{(M)}, i = 1, 2, \dots, M$, be identically distributed independent zero mean random variables with covariance: σ_F^2 . Also let the real and imaginary parts of $\Delta s_i^{(M)}$ be identically distributed and independent. If we substitute Eq. (A2) into Eq. (A1) and take the expected value, the first term of Eq. (A1) is zero because the Δs_i is zero mean and the following expression results:

$$E\{\Delta P_{in}\} = \int_{-\infty}^{\infty} |H|^2 E \left\{ \left| \sum_{i=1}^M \frac{\Delta s_i^{(M)}}{j\omega - s_i} \right|^2 \right\} d\omega. \quad (A3)$$

If we rewrite the summation by expanding the magnitude in Eq. (A3) and evaluate the expected values of the cross terms (many are equal to zero), then Eq. (A3) can be simplified to

$$E\{\Delta P_{in}\} = \sigma_F^2 \sum_{i=1}^M \int_{-\infty}^{\infty} \frac{|H|^2 d\omega}{|j\omega - s_i|^2}. \quad (A4)$$

2. *The $E\{\mathbf{r}_0^T \mathbf{R}_0^{-1} \Delta \mathbf{R} \mathbf{R}_0^{-1} \mathbf{r}_0\}$ Term:*

Because $\mathbf{R}_0^{-1} \mathbf{r}_0 = (0, 0, \dots, 1, 0, \dots, 0)^T$ where the 1 is in the N_2 position (the middle), the evaluation of this term reduces to just finding the expected value of the center element of $\Delta \mathbf{R}$. From Eq. (3.18), it follows that

$$\Delta R_{N_2 N_2} = \int_{-\infty}^{\infty} |H|^2 (\Delta H_A + \Delta H_A^*) d\omega + \int_{-\infty}^{\infty} |H|^2 |\Delta H_A|^2 d\omega. \quad (A5)$$

Now

$$\Delta H_A(j\omega) = \sum_{i=1}^M \frac{\Delta s_i^{(A)}}{j\omega - s_i}. \quad (A6)$$

The $\Delta s_i^{(A)}$ have the same kind of statistics as $\Delta s_i^{(M)}$. The forms of Eqs. (A5) and (A6) are identical to Eqs. (A1) and (A2), so that it follows from our previous derivation that

$$E\{\mathbf{r}_0^T \mathbf{R}_0^{-1} \Delta \mathbf{R} \mathbf{R}_0^{-1} \mathbf{r}_0\} = E\{\Delta P_{in}\}. \quad (A7)$$

The expression for $E\{\Delta P_{in}\}$ is given by Eq. (A4).

3. The $E\{\mathbf{r}_0^t \mathbf{R}_0^{-1} \Delta \mathbf{R} \mathbf{R}_0^{-1} \Delta \mathbf{R} \mathbf{R}_0^{-1} \mathbf{r}_0\}$ Term:

We can write

$$\mathbf{r}_0^t \mathbf{R}_0^{-1} \Delta \mathbf{R} \mathbf{R}_0^{-1} \Delta \mathbf{R} \mathbf{R}_0^{-1} \mathbf{r}_0 = (\mathbf{R}_0^{-1} \mathbf{r}_0)^t \Delta \mathbf{R} \mathbf{R}_0^{-1} \Delta \mathbf{R} (\mathbf{R}_0^{-1} \mathbf{r}_0). \quad (\text{A8})$$

Since $\mathbf{R}_0^{-1} \mathbf{r}_0 = (0, 0, \dots, 1, 0, \dots, 0)^T$, the expected value of the above is equal to the expected value of the center element of the matrix, $\Delta \mathbf{R} \mathbf{R}_0^{-1} \Delta \mathbf{R}$. It is straightforward to show that

$$E\{(\mathbf{R}_0^{-1} \mathbf{r}_0)^t \Delta \mathbf{R} \mathbf{R}_0^{-1} \Delta \mathbf{R} (\mathbf{R}_0^{-1} \mathbf{r}_0)\} = \sum_{k=1}^N \sum_{m=1}^N R^{(km)} E\{\Delta R_{N_2 k} \Delta R_{m N_2}\}. \quad (\text{A9})$$

If we use expressions for $\Delta R_{N_2 k}$ and $\Delta R_{m N_2}$ by using Eq. (3.18), we find that

$$E\{\Delta R_{N_2 k} \Delta R_{m N_2}\} = E \left\{ \int_{-\infty}^{\infty} |H|^2 (\Delta H_A + \Delta H_A^*) e^{j\omega\pi BT(N_2 - k)} d\omega \cdot \int_{-\infty}^{\infty} |H|^2 (\Delta H_A + \Delta H_A^*) e^{j\omega\pi BT(m - N_2)} d\omega \right\} + E\{O(\Delta H_A^2)\}. \quad (\text{A10})$$

If we evaluate only the first term of Eq. (A10) by substituting Eq. (A6) into Eq. (A10), and use the fact that

$$E\{\Delta s_i^2\} = 0, \quad (\text{A11})$$

then it can be shown that

$$E\{\Delta R_{N_2 k} \Delta R_{m N_2}\} = 2\sigma_F^2 \sum_{i=1}^M \left[\int_{-\infty}^{\infty} \frac{|H|^2 e^{j\omega\pi BT(N_2 - k)}}{j\omega - s_i} d\omega \cdot \int_{-\infty}^{\infty} \frac{|H|^2 e^{j\omega\pi BT(m - N_2)}}{-j\omega - s_i^*} d\omega \right]. \quad (\text{A12})$$

Hence by substituting Eq. (A12) into Eq. (A9), Eq. (3.39) results.

4. The $E\{\mathbf{r}_0^t \mathbf{R}_0^{-1} \Delta \mathbf{R} \mathbf{R}_0^{-1} \Delta \mathbf{r}\}$ Term:

We write

$$\mathbf{r}_0^t \mathbf{R}_0^{-1} \Delta \mathbf{R} \mathbf{R}_0^{-1} \Delta \mathbf{r} = (\mathbf{R}_0^{-1} \mathbf{r}_0)^t \Delta \mathbf{R} \mathbf{R}_0^{-1} \Delta \mathbf{r}. \quad (\text{A13})$$

The term $\Delta \mathbf{R} \mathbf{R}_0^{-1} \Delta \mathbf{r}$ is a vector and because of Eq. (3.10), the above expected value is simply the expected value of the center element of this vector. Thus, we can show that

$$E\{\mathbf{r}_0^t \mathbf{R}_0^{-1} \Delta \mathbf{R} \mathbf{R}_0^{-1} \Delta \mathbf{r}\} = \sum_{m=1}^N \sum_{k=1}^N \mathbf{R}_0^{(km)} E\{\Delta R_{N_2 k} \Delta r_m\}. \quad (\text{A14})$$

If we substitute the forms of $\Delta R_{N_2 k}$ and Δr_m given by Eqs. (3.18) and (3.19) respectively, we find that

$$E\{\Delta R_{N_2 k} \Delta r_m\} = E \left\{ \int_{-\infty}^{\infty} |H|^2 (\Delta H_A + \Delta H_A^*) e^{j\omega\pi BT(N_2 - k)} d\omega \cdot \int_{-\infty}^{\infty} |H|^2 \Delta H_A^* e^{j\omega\pi BT(m - N_2)} d\omega \right\} + E\{O(\Delta H_A \Delta H_M)\}. \quad (\text{A15})$$

The last term in Eq. (A15) is equal to zero, and the first term can be evaluated to be

$$E\{\Delta R_{N_2 k} \Delta r_m\} = \sigma_F^2 \sum_{i=1}^M \left[\int_{-\infty}^{\infty} \frac{|H|^2 e^{j\omega\pi BT(N_2 - k)}}{j\omega - s_i} d\omega \cdot \int_{-\infty}^{\infty} \frac{|H|^2 e^{j\omega\pi BT(m - N_2)}}{-j\omega - s_i^*} d\omega \right]. \quad (\text{A16})$$

Thus Eq. (A16) is substituted into Eq. (A14) and Eq. (3.32) follows.

5. *The $E\{\Delta \mathbf{r}' \mathbf{R}_0^{-1} \Delta \mathbf{R} \mathbf{R}_0^{-1} \mathbf{r}_0\}$ Term:*

By examination of Eqs. (A14) and (A16), and the fact that $R_0^{(mk)} = R_0^{(km)*}$, we can show that

$$R_0^{(mk)} E\{\Delta R_{N_2 m} \Delta r_k\} = \left[R_0^{(km)} E\{\Delta R_{N_2 k} \Delta r_m\} \right]^*. \quad (\text{A17})$$

Hence, it follows that the expression given in Eq. (3.32) is real because every term of Eq. (A14) is either real or has an associated complex conjugate term. Hence, $E\{\Delta \mathbf{r}' \mathbf{R}_0^{-1} \Delta \mathbf{R} \mathbf{R}_0^{-1} \mathbf{r}_0\}$ can be found by using the expression for $E\{\mathbf{r}_0' \mathbf{R}_0^{-1} \Delta \mathbf{R} \mathbf{R}_0^{-1} \Delta \mathbf{r}\}$ previously given.

6. *The $E\{\Delta \mathbf{r}' \mathbf{R}_0^{-1} \Delta \mathbf{r}\}$ Term:*

We can show that

$$E\{\Delta \mathbf{r}' \mathbf{R}^{-1} \Delta \mathbf{r}\} = \sum_{k=1}^N \sum_{m=1}^N \mathbf{R}_0^{(km)} E\{\Delta r_k * \Delta r_m\}. \quad (\text{A18})$$

Using the definitions of the $\Delta \mathbf{r}$ elements given by Eq. (3.19) and multiplying out these expressions we obtain

$$\begin{aligned} E\{\Delta r_k * \Delta r_m\} &= E \left\{ \int_{-\infty}^{\infty} |H|^2 \Delta H_A e^{j\omega\pi BT(N_2-k)} d\omega \right. \\ &\quad \left. \cdot \int_{-\infty}^{\infty} |H|^2 \Delta H_A * e^{j\omega\pi BT(m-N_2)} d\omega \right\} \\ &+ E \left\{ \int_{-\infty}^{\infty} |H|^2 \Delta H_M * e^{j\omega\pi BT(N_2-k)} d\omega \right. \\ &\quad \left. \cdot \int_{-\infty}^{\infty} |H|^2 \Delta H_M e^{j\omega\pi BT(m-N_2)} d\omega \right\} + E\{O(\Delta H_A \Delta H_M)\}. \end{aligned} \quad (\text{A19})$$

The last term in Eq. (A19) equals zero. Because of the identical statistics of ΔH_A and ΔH_M , the first two terms are equal. Thus, we can evaluate the above as

$$E\{\Delta r_k * \Delta r_m\} = 2\sigma_F^2 \sum_{i=1}^M \left[\int_{-\infty}^{\infty} \frac{|H|^2 e^{j\omega\pi BT(N_2-k)} d\omega}{j\omega - s_i} \int_{-\infty}^{\infty} \frac{|H|^2 e^{j\omega\pi BT(m-N_2)} d\omega}{-j\omega - s_i^*} \right]. \quad (\text{A20})$$

Appendix B EVALUATION OF INTEGRALS

In this appendix, we evaluate the integrals seen in Eqs. (3.35) and (3.36) for when the FTF is a Butterworth filter. Expressions for these integrals were listed in Eqs. (4.5) to (4.7). These integrals can be derived by using the Theory of Residues [2].

First, we find an expression for $H(s)H(-s)$ which is consistent with Eqs. (4.1) and (4.3). It is easily shown that

$$H(s)H(-s) = \frac{1}{1 + (-1)^M s^{2M}}. \quad (\text{B1})$$

Next, the poles of $H(s)H(-s)$ are identified. These poles lie on the unit circle and are equally spaced in angle (see Fig. 4.2). We can show that the right-hand plane poles are given by the expression

$$p_i^{(R)} = j e^{-j\frac{\pi}{2M}(2i-1)}, \quad i = 1, 2, \dots, M \quad (\text{B2})$$

and the left-hand plane poles are given by the expression

$$p_i^{(L)} = j e^{j\frac{\pi}{2M}(2i-1)}, \quad i = 1, 2, \dots, M. \quad (\text{B3})$$

Note that the expressions do not depend on whether M is even or odd as does $H(s)H(-s)$ and that there are no poles on the imaginary axis (the $j\omega$ axis). We set the poles of $H(s)$ equal to the left-hand plane poles:

$$s_i = p_i^{(L)}, \quad i = 1, 2, \dots, M. \quad (\text{B4})$$

In Fig. B1, we designate the path of integration of the integrals seen in Eqs. (3.35) and (3.36) as contour C_1 ; i.e., $-j\infty < j\omega < j\infty$. In addition, we have shown two other contours: C_2 and C_3 . Let $K(s)$ be the kernel of any of the integrals to be evaluated. We can then write

$$\int_{C_1} K(s) ds = \int_{C_1 + C_2} K(s) ds - \int_{C_2} K(s) ds \quad (\text{B5})$$

or

$$\int_{C_1} K(s) ds = \int_{C_1 + C_3} K(s) ds - \int_{C_3} K(s) ds. \quad (\text{B6})$$

Depending on the kernel, we can show that as $R_c \rightarrow \infty$ then either both the C_2 and C_3 contour integrals go to zero, or one goes to zero and the other goes to infinity. In our evaluation, we always choose the one that goes to zero so that we can form a closed contour about either the right-side plane poles (contour $C_1 + C_2$) or left-side plane poles (contour $C_1 + C_3$) and thus use the Theory of Residues.

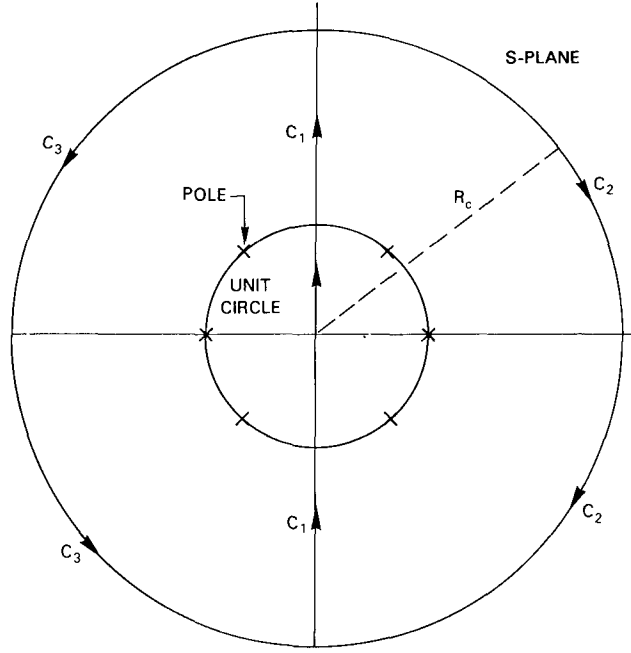


Fig. B1 — Contours of integration

1. Derivation of Eq. (4.5)

We can show for $m \leq n$

$$\begin{aligned} \int_{-\infty}^{\infty} |H(j\omega)|^2 e^{j\omega\pi BT(n-m)} d\omega &= \frac{1}{j} \oint_{C_1 + C_3} \frac{c_0 e^{s\pi BT(n-m)} ds}{1 + (-1)^M s^{2M}} \\ &= 2\pi \sum_{i=1}^M \text{Res}_i \end{aligned} \quad (\text{B7})$$

where Res_i are the M residues of the above kernel about the poles in the left-hand plane. Note we have used the fact that the integral along C_3 as seen in Eq. (B6) goes to zero as $R_c \rightarrow \infty$. All the poles are single poles. It can be shown by use of the Theory of Residues that

$$\text{Res}_i = \lim_{s \rightarrow p_i^{(L)}} \left\{ \frac{c_0 e^{s\pi BT(n-m)} (s - p_i^{(L)})}{1 + (-1)^M s^{2M}} \right\} \quad (\text{B8})$$

or evaluating the above limit

$$\text{Res}_i = -\frac{c_0}{2M} p_i^{(L)} e^{p_i^{(L)}\pi BT(n-m)}. \quad (\text{B9})$$

Substituting Eq. (B3) into Eq. (B9) and then substituting Eq. (B9) into Eq. (B7) results in Eq. (4.5b). Note we have substituted l for i in Eq. (4.5b).

We can also show for $m > n$ that

$$\int_{-\infty}^{\infty} |H(j\omega)|^2 e^{j\omega\pi BT(n-m)} d\omega = \frac{1}{j} \oint_{C_1 + C_2} \frac{c_0 e^{s\pi BT(n-m)} ds}{1 + (-1)^M s^{2M}} = -2\pi \sum_{i=1}^M \text{Res}_i \quad (\text{B10})$$

where Res_i are the M residues of the above kernel. We used the fact that the integral along C_2 seen in Eq. (B5) goes to zero as $R_c \rightarrow \infty$.

It can be shown that

$$\text{Res}_i = \lim_{s \rightarrow p_i^{(R)}} \left\{ \frac{c_0 e^{s\pi BT(n-m)} (s - p_i^{(R)})}{1 + (-1)^M s^{2M}} \right\} \quad (\text{B11})$$

or evaluating the above limit

$$\text{Res}_i = -\frac{c_0}{2M} p_i^{(R)} e^{p_i^{(R)}\pi BT(n-m)}. \quad (\text{B12})$$

Substituting Eq. (B2) into Eq. (B12) and then substituting Eq. (B12) into Eq. (B10) results in Eq. (4.5a). Again we have set $l = i$ in Eq. (4.5a).

2. Derivation of Eq. (4.6)

We can show that

$$\begin{aligned} \int_{-\infty}^{\infty} \frac{|H(j\omega)|^2 d\omega}{|j\omega - s_i|^2} &= \frac{1}{j} \oint_{C_1 + C_2} \frac{c_0 ds}{(1 + (-1)^M s^{2M})(s - s_i)(-s - s_i^*)} \\ &= -2\pi \sum_{m=1}^M \text{Res}_m \end{aligned} \quad (\text{B13})$$

where Res_m $m = 1, 2, \dots, M$ are the residues of the above kernel. Again we have used the fact that the integral along C_2 seen in Eq. (B5) goes to zero as $R_c \rightarrow \infty$. All of the poles (in the right-hand plane) of this kernel are single poles except when $i = m$ or

$$p_i^{(R)} = -s_i \quad (\text{B14})$$

which results in a double pole.

For the single poles, $m \neq i$, we can show

$$\text{Res}_m = \lim_{s \rightarrow p_m^{(R)}} \left\{ c_0 \frac{s - p_m^{(R)}}{(1 + (-1)^M s^{2M})(s - s_i)(-s - s_i^*)} \right\}. \quad (\text{B15})$$

We can show using l'Hopital rule that

$$\begin{aligned} \text{Res}_m &= \frac{c_0}{2M} \frac{1}{p_m^{(R)} - p_m^{(R)*} + s_i^* - s_i} \\ &= -\frac{j c_0}{4M} \frac{1}{\cos \frac{\pi}{2M} (2m-1) - \cos \frac{\pi}{2M} (2i-1)}. \end{aligned} \quad (\text{B16})$$

Since all of the Res_m , for $m \neq i$, are purely imaginary and we know that the integral to be evaluated is real, these terms will cancel out with the imaginary part of Res_i . We can show that

$$\text{Res}_i = \lim_{s \rightarrow -s_i^*} \left\{ \frac{d}{ds} \left[-c_0 \frac{s + s_i^*}{(1 + (-1)^M s^{2M})(s - s_i)} \right] \right\}. \quad (\text{B17})$$

After taking the derivative and applying l'Hopital rule twice, we find that

$$\begin{aligned} \text{Res}_i &= \frac{c_0}{2} \frac{c_0}{s_i + s_i^*} + \frac{1}{4M} \frac{s_i^* - s_i}{(s_i + s_i^*)^2} \\ &= -\frac{c_0}{4} \frac{1}{\sin \frac{\pi}{2M} (2i-1)} - j \frac{c_0}{8M} \frac{\cos \frac{\pi}{2M} (2i-1)}{\sin^2 \frac{\pi}{2M} (2i-1)}. \end{aligned} \quad (\text{B18})$$

Adding all the residues and evaluating Eq. (B13) results in Eq. (4.6).

3. Derivation of Eq. (4.7)

It can be shown that for $k \leq n$

$$\begin{aligned} \int_{-\infty}^{\infty} \frac{|H(j\omega)|^2 e^{j\omega\pi BT(k-n)} d\omega}{j\omega - s_i} &= \frac{1}{j} \oint_{C_1 + C_2} \frac{c_0 e^{s\pi BT(k-n)} ds}{(1 + (-1)^M s^{2M})(s - s_i)} \\ &= -2\pi \sum_{m=1}^M \text{Res}_m \end{aligned} \quad (\text{B19})$$

where $\text{Res}_m, m = 1, 2, \dots, M$ denotes the residues of the above kernel. All of the poles are single poles. We can show that

$$\text{Res}_m = \lim_{s \rightarrow p_m^{(R)}} \left\{ c_0 \frac{(s - p_m^{(R)}) e^{s\pi BT(k-n)}}{(1 + (-1)^M s^{2M})(s - s_i)} \right\} \quad (\text{B20})$$

$$= -\frac{c_0}{2M} \frac{p_m^{(R)}}{p_m^{(R)} - s_i} e^{p_m^{(R)}(k-n)\pi BT}. \quad (\text{B21})$$

If Eq. (B2) is substituted into Eq. (B21) and then Eq. (B21) is substituted into Eq. (B19), then Eq. (4.7a) results with $k = N_2$.

For $k > n$, we can show that

$$\begin{aligned} \int_{-\infty}^{\infty} \frac{|H(j\omega)|^2 e^{j\omega\pi BT(k-n)} d\omega}{j\omega - s_i} &= \frac{1}{j} \oint_{C_1 + C_3} \frac{c_0 e^{s\pi BT(k-n)} ds}{(1 + (-1)^M s^{2M})(s - s_i)} \\ &= 2\pi \sum_{m=1}^M \text{Res}_m \end{aligned} \quad (\text{B22})$$

where $\text{Res}_m, m = 1, 2, \dots, M$ are the residues of the above kernel. This kernel has $M - 1$ single poles and one double pole for when $m = i$. For $m \neq i$, we can show that

$$\begin{aligned} \text{Res}_m &= \lim_{s \rightarrow p_m^{(L)}} \left\{ c_0 \frac{(s - p_m^{(L)}) e^{s\pi BT(k-n)}}{(1 + (-1)^M s^{2M})(s - s_i)} \right\} \\ &= -\frac{c_0}{2M} \frac{e^{\frac{\pi BT(k-n)}{2M} (2m-1)} e^{j\pi BT(k-n) \cos \frac{\pi}{2M} (2m-1)}}{1 - e^{j\frac{\pi}{M} (i-m)}}. \end{aligned} \quad (\text{B23})$$

For $i = m$, we can show that

$$\text{Res}_i = \lim_{s \rightarrow s_i} \frac{d}{ds} \left\{ \frac{(s - s_i) e^{s\pi BT(k-n)}}{1 + (-1)^N s^{2M}} \right\}. \quad (\text{B24})$$

After taking the derivative and applying l'Hopital rule twice, the following expression results:

$$\text{Res}_i = \frac{1}{2M} \left(M - .5 - BT(k-n) \right) j e^{j \frac{\pi}{2M} (2i-1)} e^{-\pi BT(k-n) \sin \frac{\pi}{2M} (2i-1)} \cdot e^{j\pi BT(k-n) \cos \frac{\pi}{2M} (2i-1)}. \quad (\text{B25})$$

Substituting Eqs. (B23) and (B25) in Eq. (B22) results in Eq. (4.7b) with $k = N_2$.